Solar-Terrestrial Physics. 2023. Vol. 9. Iss. 4. P. 123–135. DOI: 10.12737/stp-94202315. © 2023 V.I. Mordvinov, E.V. Devyatova, V.M. Tomozov. Published by INFRA-M Academic Publishing House

UDC 551.51, 532.5
DOI: 10.12737/stp-94202315

Received June 16, 2023
Accepted October 10, 2023

INFLUENCE OF THE MAGNETIC FIELD AND THE MEAN FLOW CONFIGURATION ON SPATIAL STRUCTURE AND GROWTH RATE OF NORMAL MODES

V.I. Mordvinov
Institute of Solar-Terrestrial Physics SB RAS, Irkutsk, Russia, v_mordv@iszf.irk.ru

E.V. Devyatova
Institute of Solar-Terrestrial Physics SB RAS, Irkutsk, Russia, devyatova@iszf.irk.ru

V.M. Tomozov
Institute of Solar-Terrestrial Physics SB RAS, Irkutsk, Russia, tom@iszf.irk.ru

Abstract. The first part of the work presents the results of numerical experiments with the magnetohydrodynamic model of “shallow water” to assess the degree of influence of the magnetic field on the development of instabilities conditioned by a combination of inhomogeneities in the mean flow and the mean magnetic field. Normal mode calculations have confirmed the earlier obtained result on the different influence of weak and strong magnetic fields on the instability of differential rotation. Calculations have shown that a weak magnetic field stabilizes the development of instabilities, whereas a strong magnetic field, on the contrary, enhances the instability. Azimuthal inhomogeneities of differential rotation in all cases contribute to the development of instabilities. In the second part of the work, we examine the spatial structure of normal modes and make an attempt to interpret the torsional oscillations observed in the atmospheres of Earth and the Sun. Calculations have shown that regular axisymmetric disturbances can be caused by the formation of a cyclonic vortex above the pole, which is characteristic of Earth's atmosphere and, possibly, of the Sun's atmosphere. The least damped normal mode of a stable polar cyclone has a structure of torsional oscillations. Flow anomalies and the development of an anticyclonic eddy in winter at midlatitudes destroy torsional oscillations and lead to a rapid amplification of normal modes, which are more complex in structure.

Keywords: hydrodynamics, atmosphere, normal modes, magnetic field, torsional oscillations.

INTRODUCTION

Of particular interest in geophysical hydrodynamics are the generation mechanisms of large-scale fields and their spatial structure on time scales exceeding the rotation periods of astrophysical objects. Some anomalies of large-scale fields are formed under external forcing such as forcing of radiative and thermal energy to planetary atmospheres, yet some field anomalies are not directly related to external forcing, they are due to the internal dynamics of the environment. In Earth's atmosphere, these are quasi-stationary North Atlantic and North Pacific Lows, subtropical anticyclones in the troposphere, blockings, stratospheric polar vortices, traveling waves with periods of 4, 5, 10, 16, 25... days, etc. [Large-scale, 1988; Branstator, Held, 1995]; in the Sun, large-scale magnetic fields associated with complexes of activity on the Sun, active longitudes in sunspot activity, and solar cyclicity [Miesch, 2005; Bumba, 1979; Bumba, Makarov, 1989; Bumba, Howard, 1965; Tikhomolov, 2005; Mordvinov et al., 2012, 2013]. There is no consensus on the generation mechanisms of these anomalies. Some of them may result from generation of normal modes; others, from the development of nonlinearity, for example, Rossby wave breaking (atmospheric blocking anticyclones), traveling and stationary wave interaction [Large-scale, 1988].

Generation of large-scale magnetic field anomalies on the Sun most likely occurs in the tachocline, a thin shear layer between radiative and convective zones [Cally et al., 2003; Dikpati, Gilman, 2001; Gilman et al., 2007]. At supercritical horizontal velocity gradients and subcritical vertical temperature gradients, two-dimensional turbulence can develop in this layer; which transfers the energy of disturbances toward small wave numbers. This effect is well known both on the Sun and in Earth's atmosphere [Miesch, 2005; Danilov, Gurari, 2000]. A number of studies have assessed the magnetic field effect on the growth rate of instability [Cally et al., 2003; Dikpati, Gilman, 2001; Gilman et al., 2007; Gilman, Fox, 1997]. Calculations have shown that instability increases with increasing mean magnetic field. Nonetheless, according to other estimates, the magnetic field should stabilize the flow [Mishin, Tomozov, 2014]. Whether these contradictory views can be reconciled is still an open question. Our numerical experiments in an evolutionary model with a frozen-in magnetic field have demonstrated that such a possibility exists: weak fields can stabilize the flow, whereas strong fields can disturb it [Mordvinov et al., 2019]. However, numerical calculations of flow dynamics depend on many parameters: time and space steps, number of harmonics in expansion, the spatial structure of dis-

turbances at a reference time, and the spatial structure of mean flow. This paper is a sequel to the studies initiated by Mordvinov et al. [2019]; however, instead of complex numerical calculations of flow dynamics, we employ a simpler and widely-accepted method of normal modes [Dymnikov, Skiba 1986; Dymnikov, Filatov 1988].

In this method, the velocity field and magnetic field disturbances are given as the product of an exponent by an arbitrary function of spatial coordinates

$$\psi'(\lambda, \mu, t) = e^{\sigma t}\psi_0(\lambda, \mu),$$

$$\chi'(\lambda, \mu, t) = e^{\sigma t}\chi_0(\lambda, \mu),$$

where λ is the longitude; μ=cosθ, θ is the polar angle, and are substituted in a linearized system of equations. These oscillations are called normal modes. The coefficients σ and the functions ψ_0, χ_0 characterizing normal modes are generally complex and are calculated by solving the eigenvalue problem of a linear operator. The normal mode is growing at $\mathrm{Re}(\sigma) > 0$, damped at $\mathrm{Re}(\sigma) < 0$, neutral at $\mathrm{Re}(\sigma) = 0$, and stationary at $\mathrm{Im}(\sigma) = 0$. At each point in space, the mode describes a harmonic oscillation with the same period, but different amplitudes and initial phases. The values of σ, ψ_0, χ_0 depend on the physical parameters of the problem: the spatial structure of mean flow, the structure of mean magnetic field, fluid viscosity, and magnetic viscosity.

Unlike the studies that only examined the stability of axisymmetric flows on the Sun, for example, numerous studies by Gilman and co-authors [Dikpati, Gilman, 2001; Dikpati, Gilman, 2005; Gilman, 1967; Gilman, Fox, 1997; Gilman et al., 2007], we also take into account the influence of the azimuthal inhomogeneities of the stationary mean flow and of the stationary mean magnetic field, which may be generated by penetrating convection and/or relic magnetic field, on the development of instability of longitudinal inhomogeneities. This, in addition to the proposed analysis method, is the novelty of our work.

On large spatial scales, Earth's atmosphere is convectively stable, as is the tachocline on the Sun, but it is horizontally inhomogeneous, especially in the region of jet streams; therefore, both stationary large-scale anomalies such as subtropical anticyclones or polar vortices and traveling disturbances can be generated in it: Rossby waves at midlatitudes, Kelvin waves, planetary gravity waves in the tropics [Gill, 1986]. Interesting objects are regular oscillations in the velocity, pressure, and temperature fields with periods 5–25 days [Mordvinov, Latysheva, 2013; Zorkaltseva et al., 2019], identified after pre-filtration and zonal averaging. The oscillations propagate in the meridional direction over long distances. We call these oscillations torsional by analogy with similar oscillations on the Sun. Using one-point correlations with time lag, the spatial structure and dynamics of oscillations have been established, but their origin has not yet been clarified. Torsional oscillations on the Sun are well known [Altrock et al., 2006]. The universality of this phenomenon suggests that it is based on some common properties of large-scale hydrodynamic flows. In [Mordvinov and Zorkaltseva, 2022], we drew attention to the fact that the structure of torsional oscillations resembles the structure of one of the normal modes with a fairly realistic configuration of the mean flow. In this paper, we continue this research.

In the first part of this paper, we examine the degree of axisymmetric flow instability with the differential rotation profile of the Sun, proposed in [Kitchatinov, Rüdiger, 2009], and the non-axisymmetric flow, as in [Mordvinov et al., 2013], taking into account the magnetic field.

In the second part, we study the spatial structure of normal modes of the flow, conditioned by the combination of a polar cyclonic vortex and an anticyclonic vortex at midlatitudes. In a stylized form, this combination is representative of large-scale features of stratospheric flows. Prominence is given to axisymmetric modes resembling torsional oscillations [Zorkaltseva et al., 2019].

STABILITY OF FLUID FLOW WITH A MAGNETIC FIELD MODEL

To describe the hydrodynamic component of the flow, we use a barotropic quasi-geostrophic numerical model [Dikpati, Gilman, 2001]. In atmospheric physics, models of this type are applied to teleconnections, Rossby waves, low-frequency oscillations (North Atlantic Oscillation, Arctic/Antarctic Oscillations), conditions of occurrence and dynamics of large-scale anomalies in the atmosphere, interhemispheric interactions [Large-scale, 1988]. It is especially worthwhile using the two-dimensional quasi-geostrophic models for the stratosphere, where there is no vertical convection, and the horizontal scale of anomalies of meteorological fields is significantly larger than in the troposphere [Gill, 1986].

To study the Sun, the Lorentz force is included in the hydrodynamic model and the vortex equation is complemented by the equation of magnetic field dynamics. Further transformations depend on the purpose and method of research. For example, Fournier et al. [2022] employ a similar model to estimate the effect of viscosity on planetary waves. To examine the initial development of instability, the resulting system of equations is linearized, and either numerical computing of the evolution of disturbances are made or normal mode characteristics are calculated [Dikpati, Gilman, 2001; Dikpati, Gilman, 2005; Gilman, Fox, 1997]. In [Mordvinov et al., 2019], we followed the former method, and now we adopt the latter one, which is simpler and more universal.

The hydrodynamic model is based on the equation of quasi-geostrophic potential vortex

$$\frac{\partial(L\psi)}{\partial t} = -\frac{1}{R^2}J(\psi, \Delta\psi) - \frac{2\Omega}{R^2}\frac{\partial\psi}{\partial\lambda} - \\ -r\Delta\psi - K\Delta^3(\Delta\psi) - f(\psi), \qquad (1)$$

where $J(f, g) \equiv \frac{\partial f}{\partial\lambda}\frac{\partial g}{\partial\mu} - \frac{\partial f}{\partial\mu}\frac{\partial g}{\partial\lambda}$ is the Jacobi operator;

$L\psi \equiv \left(\Delta - L_{\mathrm{D}}^{-2}\right)\psi$; R is the solar radius; ψ is the stream function; l=2Ωμ is the Coriolis parameter; Ω is the angular velocity of the Sun; $L_{\mathrm{D}} \equiv \sqrt{gh_0}/l \approx \sqrt{gh_0}/\left(2\Omega \sin 45^\circ\right)$ is the Rossby — Obukhov deformation radius; h_0 is the average thickness of a homogeneous fluid layer; λ is the longitude; μ=cosθ; θ is the polar angle; $r=1/T_0$ is the Rayleigh friction coefficient; K is the turbulent hyperviscosity coefficient. The value of K is chosen so that the third degree hyperviscosity is equal to the usual turbulent viscosity for the dipole harmonic of a stream function expansion in harmonics [Mordvinov et al., 2013]. The function $f(\psi)$ characterizes the forcing caused by small-scale vortices.

If the stationary solution of the equation is known, f can be determined from the relation

$$f = G(\overline{\psi}) = -\frac{1}{R^2}\left[J(\overline{\psi}, \Delta\overline{\psi}) + J(\overline{\psi}, lh_{\mathrm{T}}/h_0)\right] - \\ -\frac{2\Omega}{R^2}\frac{\partial\overline{\psi}}{\partial\lambda} - r\Delta\overline{\psi} - K\Delta^3(\Delta\overline{\psi}).$$

In this case, the original equation takes the form

$$\frac{\partial(L\psi)}{\partial t} = G(\psi) - G(\overline{\psi}).$$

Since the Jacobi operator is nonlinear,

$$G(\psi) - G(\overline{\psi}) \neq G(\psi - \overline{\psi}).$$

It can be simplified if the stationary solution of the vortex equation has zonal or meridional symmetry. In this case, Jacobi operators are zero and only linear terms remain in the expression for f.

If a fluid is magnetized, the vertical component of the Lorentz force vortex must be included in Equation (1). If a magnetic field is horizontal and div(**H**)=0, the expression for this component takes the form [Mordvinov et al., 2019]

$$\mathrm{rot}\left[(\nabla\times\mathbf{H})\times\mathbf{H}\right]_z = (\mathbf{H}\nabla)\,\mathrm{rot}\,\mathbf{H}_z = (\mathbf{H}\nabla)\Delta\chi, \qquad (2)$$

where χ is the magnetic stream function related to the horizontal magnetic field vector **H** by the relation

$$\mathbf{H} = \mathbf{k}\times\nabla\chi = \left(-\mathbf{i}\frac{\partial\chi}{\partial y}, \mathbf{j}\frac{\partial\chi}{\partial x}, 0\right).$$

In the absolute Gaussian units (centimeter—gram—second), the coefficient k_0 is $1/(4\pi\rho)$, the magnetic field induction is measured in Gauss. Since the plasma density is assumed to be constant, we introduce a new variable $\chi' = \chi\sqrt{k_0}$. (the magnetic field dimension in this case will be the same as the velocity one — cm/s). At the base of the convection zone, the density $\rho \approx 10^{-2}$ g/cm^3 and the multiplier $\sqrt{k_0}$ are numerically equal

$$\sqrt{k_0} = \sqrt{1/(4\pi\rho)} = \sqrt{10^2/(4\pi)} = \sqrt{25/\pi} = 2.82.$$

Given the Lorentz force, the equation of potential vortex becomes

$$\frac{\partial(L\psi)}{\partial t} = -\frac{1}{R^2}\left[J(\psi, \Delta\psi) - J(\chi, \Delta\chi)\right] - \\ -\frac{2\Omega}{R^2}\frac{\partial\psi}{\partial\lambda} - r\Delta\psi - K\Delta^3(\Delta\psi) - G(\overline{\psi}). \qquad (3)$$

Since the velocity field is vortex-like, the equation of magnetic field induction has the form

$$\frac{\partial\mathbf{H}}{\partial t} = -(\mathbf{V}\nabla)\mathbf{H} + (\mathbf{H}\nabla)\mathbf{V} - F_{\mathrm{mp}}. \qquad (4)$$

If we take a rotor from (4) and express **H** in terms of the magnetic stream function, we obtain an equation for χ

$$\frac{\partial\Delta\chi}{\partial t} = -\frac{1}{R^2}\left\{J(\psi, \Delta\chi) - J(\chi, \Delta\psi)\right\} - \\ -r_m\Delta\chi - K_m\Delta^3(\Delta\chi). \qquad (5)$$

where r_m, K_m are magnetic viscosity parameters. Suppose that large-scale flow anomalies reflect the configurations of the fastest growing or slowest decaying low-amplitude disturbances. Represent the stream functions in the form of $\psi = \overline{\psi} + \psi'$, $\chi = \overline{\chi} + \chi'$. Taking into account the smallness of perturbations $\psi' \ll \overline{\psi}$, $\chi' \ll \overline{\chi}$,, linearize Equations (3) and (5). The equations for perturbations of ψ' and χ' take the form

$$\frac{\partial\left(\Delta - L_{\mathrm{D}}^{-2}\right)\psi'}{\partial t} = -\frac{1}{R^2}\left\{\left[J(\psi', \Delta\overline{\psi}) + J(\overline{\psi}, \Delta\psi')\right] - \right. \\ \left. -\left[J(\chi', \Delta\overline{\chi}) + J(\overline{\chi}, \Delta\chi')\right]\right\} - \frac{2\Omega}{a^2}\frac{\partial\psi'}{\partial\lambda} - \\ -r\Delta\psi' - K\Delta^3(\Delta\psi'), \qquad (6) \\ \frac{\partial\Delta\chi'}{\partial t} = -\frac{1}{R^2}\left\{\left[J(\psi', \Delta\overline{\chi}) + J(\overline{\psi}, \Delta\chi')\right] - \right. \\ \left. -\left[J(\chi', \Delta\overline{\psi}) + J(\overline{\chi}, \Delta\psi')\right]\right\} - r_{\mathrm{m}}\Delta\chi - K_{\mathrm{m}}\Delta^3(\Delta\chi).$$

where $\overline{\psi}$ and $\overline{\chi}$ are the average stream functions satisfying the system of stationary equations.

Suppose $\overline{\chi} = \alpha_1\overline{\psi}$, $\alpha_1 = const$. This means that in a stationary flow, fluid moves along magnetic field lines. Equations (6) take the form

$$\frac{\partial\left(\Delta - L_{\mathrm{D}}^{-2}\right)\psi'}{\partial t} = -\frac{1}{R^2}\left\{\left[J(\psi' - \alpha_1\chi', \Delta\overline{\psi}) + \right.\right. \\ \left.\left. +J(\overline{\psi}, \Delta(\psi' - \alpha_1\chi'))\right]\right\} - \frac{2\Omega}{R^2}\frac{\partial\psi'}{\partial\lambda} - r\Delta\psi' - \\ -K\Delta^3(\Delta\psi'), \\ \frac{\partial\Delta\chi'}{\partial t} = -\frac{1}{R^2}\left\{J((\alpha_1\psi' - \chi'), \Delta\overline{\psi}) - \right. \\ \left. -J(\overline{\psi}, \Delta(\alpha_1\psi' - \chi'))\right\} - r_{\mathrm{m}}\Delta\chi' - K_{\mathrm{m}}\Delta^3(\Delta\chi'). \qquad (7)$$

To determine α_1, use the condition: at a speed equal to 1 m/s, the coefficient must be such that the magnetic field strength is 1 G. It can be shown that in this case α_1=0.0035. In the linearized problem, the evolution of perturbations does not depend on their amplitude at a reference time, but depends on the coefficient α_1. In numerical experiments, we set the values of α_1 corresponding to the field strengths of 1, 10, 100, 1000, and 10000 G.

The dynamics of perturbations ψ', χ', determined by system of equations (7) depends on many parameters: differential rotation characteristics, the structure of the mean

flow and the mean magnetic field, turbulent viscosity, and Rayleigh friction characteristics. Examine the dependence of the mean flow instability on two parameters: the coefficient α_1 and the amplitude of differential rotation anomalies. Represent the stream function of mean flow as the sum of differential rotation and mean flow perturbation $\overline{\psi}(\mu, \lambda) = \overline{\psi}_s(\mu) + \overline{\psi}_{as}(\mu, \lambda)$. We specify the differential rotation profile in the form proposed in [Kitchatinov, Rüdiger, 2009]:

$$\Omega = \Omega_0 \left(1 - a\left((1-f)\cos^2\theta + f\cos^4\theta\right)\right), \qquad (8)$$

where Ω_0 is the differential angular velocity of the Sun at the equator, the coefficients a, f define the differential rotation profile steepness. Take the e-folding times of the Rayleigh damping to be T=500 and T=1000 rotations.

Assume that $r_m = r$, $K_m = K$. The mean flow perturbation is specified in the form of a spherical harmonic $k^* P_6^5(\mu)\cos(5\lambda)$ [Mordvinov et al., 2013]. Since the mean flow perturbation amplitude k is a relative value, Figure 1 illustrates the total distributions of the differential rotation stream function and differential rotation anomalies at the k values we use.

To analyze the mean flow instability, we represent the stream function perturbation as a normal mode [Dymnikov, Filatov, 1988], and write the functions ψ_0, χ_0 as the sum of spherical harmonics

$$\psi_0(\lambda, \mu, t) = e^{\sigma t}\sum_\gamma \psi_\gamma Y_\gamma(\mu, \lambda),$$
$$\chi_0(\lambda, \mu, t) = e^{\sigma t}\sum_\gamma \chi_\gamma Y_\gamma(\mu, \lambda), \qquad (9)$$

where σ is the complex frequency; $\gamma=(m, n)=(m_\gamma, n_\gamma)$ is the wave vector; m is the zonal wave number; n is the degree of spherical function $Y_\gamma(\lambda, \mu) = P_n^m e^{im\lambda}$. Following [Gilman, Fox, 1997], we take the complex frequency σ to be the same for hydrodynamic and magnetic disturbances, which, generally speaking, is not obvious.

Reduce Equations (7) to a dimensionless form and substitute solutions in the form (9). Take the solar radius as the length scale, and Ω^{-1} as the time scale. Introduce designations

$$r_1 = \frac{1}{\Omega}\left\{r + Kn^3(n+1)^3/a^6\right\},$$
$$k'_n = n(n+1),$$
$$k_n = \left(n(n+1) + F^2\right),$$

where $F = R/L_D$ is the Froude number. Taking into account the property of spherical functions, $\Delta Y_\gamma = -n(n+1)Y_\gamma / R^2$, after integration over a spherical surface, we obtain equations for coefficients of the stream function expansion ψ_γ, χ_γ

$$\begin{aligned} k_n\sigma\psi_\gamma &= \psi_\gamma\left(-n(n+1)r_1 + i2m\right) + \\ &+\frac{1}{\Omega}\left[\sum_\gamma\left(\psi_\gamma - \alpha_1\chi_\gamma\right)\int_S Y^*_{\gamma'} J\left(Y_\gamma, G_n\right)dS\right], \\ k'_n\sigma\chi_\gamma &= \chi_\gamma\left(n(n+1)r_1\right) + \\ &+\frac{1}{\Omega}\sum_\gamma\left(\alpha_1\psi_\gamma - \chi_\gamma\right)\int_S Y^*_{\gamma'} J\left(Y_\gamma, G'_n\right)dS. \end{aligned} \qquad (10)$$

or in the matrix form

$$\begin{aligned} A_{\gamma\gamma'}\psi_\gamma + B_{\gamma\gamma'}\chi_\gamma &= \sigma'\psi_{\gamma'}, \\ A'_{\gamma\gamma'}\psi_\gamma + B'_{\gamma\gamma'}\chi_\gamma &= \sigma'\chi_{\gamma'}, \end{aligned} \qquad (11)$$

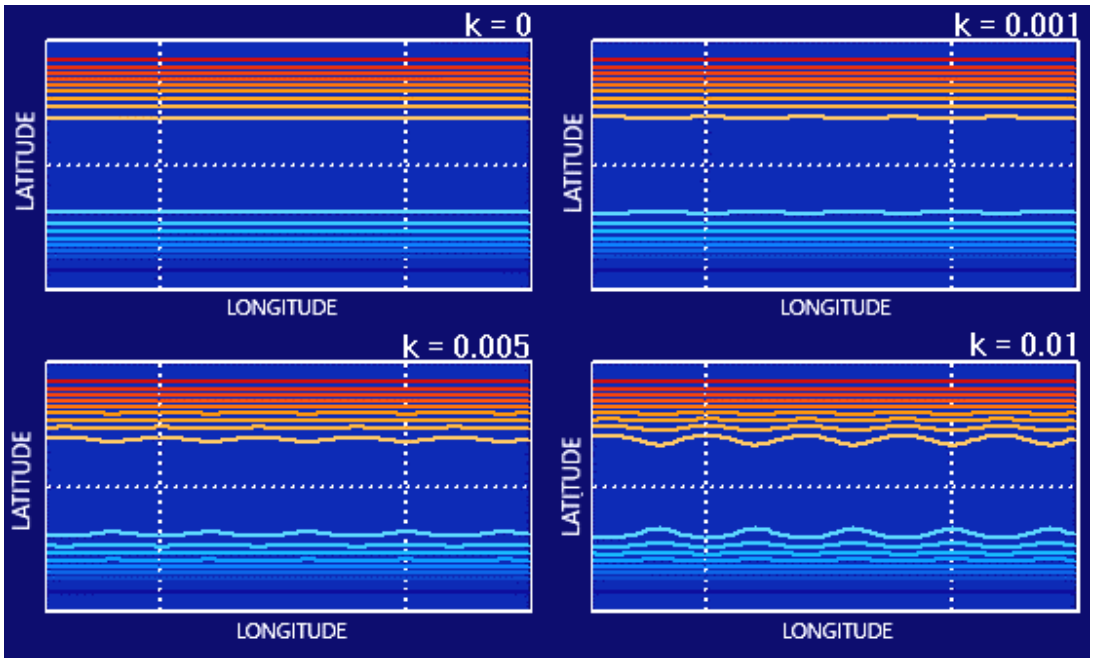

Figure 1. Stream functions of the sum of axisymmetric differential rotation and anomalies $k^* P_6^5(\mu)\cos(5\lambda)$ at different k values

where

$$A_{\gamma\gamma'} = \frac{1}{k_{n'}\Omega}\left\{\int_S Y^*_{\gamma'} J\left(Y_\gamma, G_n\right)dS\right\} + \\ +\delta_{\gamma\gamma'}\left[i2m' - r_1 n'\left(n'+1\right)\right],$$

$$B_{\gamma\gamma'} = -\frac{\alpha_1}{k_{n'}\Omega}\left\{\int_S Y^*_{\gamma'} J\left(Y_\gamma, G_n\right)dS\right\},$$

$$A'_{\gamma\gamma'} = \frac{\alpha_1}{k_{n'}\Omega}\left\{\int_S Y^*_{\gamma'} J\left(Y_\gamma, G'_n\right)dS\right\},$$

$$B'_{\gamma\gamma'} = -\frac{1}{k_{n'}\Omega}\left\{\int_S Y^*_{\gamma'} J\left(Y_\gamma, G'_n\right)dS\right\} - \delta_{\gamma\gamma'}\left[r_1 n'\left(n'+1\right)\right],$$

$$G_n = \Delta\overline{\psi} + k_n\overline{\psi},\ \ G'_n = \Delta\overline{\psi} - k_n\overline{\psi},\ \ \sigma' = \sigma/\Omega..$$

Inserting G_n G'_n in the expressions for matrix element $A_{\gamma\gamma'}$, $B_{\gamma\gamma'}$, $A'_{\gamma\gamma'}$, $B'_{\gamma\gamma'}$, we calculate double integrals, using quadratures. The λ integral is calculated by the quadrature formula of rectangles; and the μ integral, by the Gauss quadrature [Dymnikov, Skiba, 1986]:

$$\int_{-1}^{1} f(\mu)d\mu \approx \sum_{k=1}^{K} C_k\, f(\mu_k),$$

where μ_k are the roots of Legendre polynomials $P_k(\mu)$.

$$C_k = \frac{2\left(1-\mu_k\right)^2}{\left[KP_{k-1}\left(\mu_k\right)\right]^2},\ k = 1, 2, ..., K.$$

The number of nodes in the variable λ was 144; in the variable μ, 64.

If we form a block matrix

$$D = \begin{pmatrix} A_{\gamma\gamma'} & B_{\gamma\gamma'} \\ A'_{\gamma\gamma'} & B'_{\gamma\gamma'} \end{pmatrix} = \begin{pmatrix} A_{\gamma\gamma'} & \alpha B_{\gamma\gamma'} \\ \alpha_1 A'_{\gamma\gamma'} & B'_{\gamma\gamma'} \end{pmatrix}$$ and a vector $x = \begin{pmatrix} \psi_\gamma \\ \chi_\gamma \end{pmatrix}$,

system (11) can be rewritten as a matrix equation for eigenvalues and eigenfunctions of the matrix D

$$Dx = \sigma' x. \qquad (12)$$

The eigenvalues σ' determine the normal mode frequencies (complex); and the eigenvectors x, the spatial structure of normal modes. Both depend on the configuration of the mean flow and the mean magnetic field, viscosity parameterization, etc. The real part of the frequency σ' defines the normal mode amplitude increment; the imaginary part, the oscillation frequency.

The dependence of normal modes on external forcing can be studied theoretically and experimentally. One of the theoretical methods, developed by E. Schrödinger, is basically as follows [Marchuk et al., 1986]. With changing external forcing, the operator D in (12) changes, and we come to the problem

$$\tilde{D}\tilde{x} = \tilde{\sigma}\tilde{x}. \qquad (13)$$

In general, the solution of (13) requires an analysis of the spectrum of both original and perturbed operators. Suppose that the perturbation of D is determined by the parameter ε so that $\tilde{D}$ is an analytical function regular in the vicinity of the point $\varepsilon=0$:

$$\tilde{D} = \sum_{i=0}^{\infty} \varepsilon^i D^{(i)}, \qquad (14)$$

where $D^{(0)}=D$, $D^{(i)}$ are some linear operators.

The eigenvalue $\tilde{\sigma} = \sigma(\varepsilon)$ and eigenfunction $\tilde{x} = x(\varepsilon)$ of $\tilde{D}$ can also be represented as series in power of ε

$$\tilde{\sigma} \equiv \sigma(\varepsilon) = \sum_{i=0}^{\infty} \varepsilon^i \sigma^{(i)},\ \sigma^{(0)} = \sigma_0, \\ \tilde{x} \equiv x(\varepsilon) = \sum_{i=0}^{\infty} \varepsilon^i x^{(i)},\ x^{(0)} = x_0. \qquad (15)$$

Substituting the series in Equation (13), we obtain a system of equations

$$\left(D-\sigma_0 E\right)x^{(0)} = 0, \\ \left(D-\sigma_0 E\right)x^{(1)} = f_1, \qquad (16) \\ \left(D-\sigma_0 E\right)x^{(n)} = f_n,$$

in which the right-hand sides are determined by the formulas

$$f_n = \sum_{i=1}^{n} \sigma^{(i)} x^{(n-i)} - \sum_{i=1}^{n} D^{(i)} x^{(n-i)}. \qquad (17)$$

To resolve (16), the condition of orthogonality of f_n to the element x_0^* — the solution of the conjugate uniform problem — must be fulfilled $D^* x_0^* = \overline{\sigma}_0 x_0^*$:

$$\left(f_n, x_0^*\right) = 0,\ n = 1, 2, ... \qquad (18)$$

Since the eigenfunctions $x(\varepsilon)$ are found from (16) up to a multiplier, additional normalization conditions are usually introduced such as $\left(x(\varepsilon), x_0^*\right) = 1$. Relation (18) and scaling allow us to determine the expansion coefficients $\sigma(\varepsilon)$ and, using (16), the eigenfunctions $x^{(n)}$.

The Schrödinger method has long been known, but its application faces a number of problems. That is why, to assess the dependence of normal modes on external forcing, we have used numerical computing, changing the parameters of the problem and calculating eigenfunctions and eigenfrequencies of the operator.

RESULTS

Consider first the differential rotation of the Sun with parameters a=0.5, f=0.8. Table 1 lists e-folding times of the fastest growing normal modes at different amplitudes of differential rotation anomalies k and different coefficients α_1 characterizing the stationary magnetic field strength. The axisymmetric differential rotation k=0 is seen to be unstable for the selected parameters and increases e-fold for 21.15 rotations in the absence of the magnetic field. This confirms the estimates we have obtained earlier [Mordvinov et al., 2012, 2013]. We increase the magnetic field strength starting from α_1=0.0035 (1 G) to α_1=35 (10000 G). The magnetic field

Table 1

E-folding times of perturbations of differential rotation with parameters $a = 0.5$, $f = 0.8$ at different amplitudes of anomalies of differential rotation and magnetic field strength at the number of harmonics N=13 and T_0=500.

	α_1=0.0	α_1=0.0035	α_1=0.035	α_1=0.35	α_1=3.5	α_1=35
k=0	T=21.15	T=22.06	T=24.36	T=39.13	T=5.33	T=0.58
k=0.001	T=20.41	T=21.21	T=24.56	T=29.9	T=2.32	T=0.23
k=0.005	T=9.12	T=9.18	T=9.69	T=6.46	T=0.49	T=0.04
k=0.01	T=4.42	T=4.45	T=4.61	T=2.84	T=0.25	T=0.02

Table 2

E-folding times of perturbations of differential rotation with parameters a=0.5, f=0.8 at different amplitudes of anomalies of differential rotation and magnetic field strength, T_0=1000, for each value of k: in the top row, for N=13; in the bottom row, for N = 15.

	α_1=0.0	α_1=0.0035	α_1=0.035	α_1=0.35	α_1=3.5	α_1=35
k=0	T=20.71 T=20.94	T=21.58 T=21.85	T=23.77 T=26.34	T=39.63 T=23.56	T=5.44 T=2.99	T=0.59 T=0.33
k=0.001	T=19.99 T=20.20	T=20.77 T=21.06	T=23.96 T=25.98	T=30.08 T=21.89	T=2.34 T=1.66	T=0.23 T=0.15
k=0.005	T=9.04 T=5.98	T=9.09 T=6.02	T=9.60 T=6.40	T=6.46 T=5.79	T=0.49 T=0.38	T=0.04 T=0.03
k=0.01	T=4.41 T=1.77	T=4.43 T=1.78	T=4.59 T=1.99	T=2.84 T=2.94	T=0.25 T=0.19	T=0.02 T=0.01

changes the e-folding times. The field of 1, 10, 100 G slows down the development of instability, but a further 10-fold enhancement of the magnetic field reduces the e-folding time about 8 times; and at a field value of 10000 G, the growth of instabilities accelerates ~70 times. In all the cases, the amplitude of differential rotation anomalies k has a significant effect on the growth rate of perturbations. A 10-fold increase in amplitude causes the e-folding time to decrease 5–10 times. A similar dependence of instabilities on the magnetic field and the mean flow anomalies persists as friction decreases and the number of spherical harmonics in the stream function expansion increases (Table 2). When choosing the number of harmonics in the expansion, we relied on the results obtained in [Mordvinov et al., 2013], in which the dependence of the growth rates of instabilities with a change in n from 5 to 30 without a magnetic field was analyzed. A particularly strong dependence of increments of growth rate on n was recorded at n>15.

It can be seen that when a magnetic field is introduced the dependence on the number of harmonics persists.

Figure 2 exemplifies spatial distributions of the fastest growing normal modes

$$\psi'_0(\lambda,\mu) = \sum_\gamma \psi_\gamma Y_\gamma(\mu,\lambda),$$

$$\chi'_0(\lambda,\mu) = \sum_\gamma \chi_\gamma Y_\gamma(\mu,\lambda)$$

at zero amplitude of mean flow anomalies k=0, differential rotation with parameters a=0.5, f=0.8, and the time of Rayleigh damping T_0=1000 rotations of the Sun. In the stream function expansion, 13 spherical harmonics have been taken into account. The distributions are normalized to maximum values $\psi'_0(\lambda,\mu)$ and $\chi'_0(\lambda,\mu)$. Isolines from –0.9 to +0.9 are plotted. Isolines of negative stream functions are blue; and those of positive values are red. The spatial distributions of normal modes are constructed in two projections — cylindrical (on the left) and stereographic (on the right).

The spatial structures of normal modes are seen to differ greatly at different strengths of the mean magnetic field. Harmonics with large wave vectors γ generally turn out to be the most unstable. Large-scale normal modes with small γ are more stable. Of particular interest (see Figure 2) are the axisymmetric normal mode of the stream function at α_1=0.35 (100 G), (torsional oscillations) (panel *a*, the fourth distribution from above) and the dipole mode of the magnetic stream function at α_1=3.5 (1000 G) (sector structure of the photospheric magnetic field) (panel *b*, the fifth distribution from above). These modes can be compared with observations. Nonetheless, given the strong dependence of normal modes on simulation parameters, it seems premature to interpret the real large-scale structures of the magnetic field and the velocity field in terms of normal modes, at least without a case study.

Examine the differential rotation with parameters a=f=0.2. We have shown that the axisymmetric rotation with such parameters is stable without a magnetic field [Mordvinov et al., 2012, 2013]. The magnetic field and the mean flow anomalies change the situation. Tables 3, 4 present the results of calculations of e-folding times of the most unstable normal modes at α_1 from 0.0035 to 35 and different amplitudes k of mean flow anomalies. In all the cases, the flows become unstable, yet the e-folding times of the perturbation amplitude are longer than those for the differential rotation parameters a=0.5, f=0.8.

Summarize the calculations of normal modes with a frozen-in magnetic field. The calculations show that an

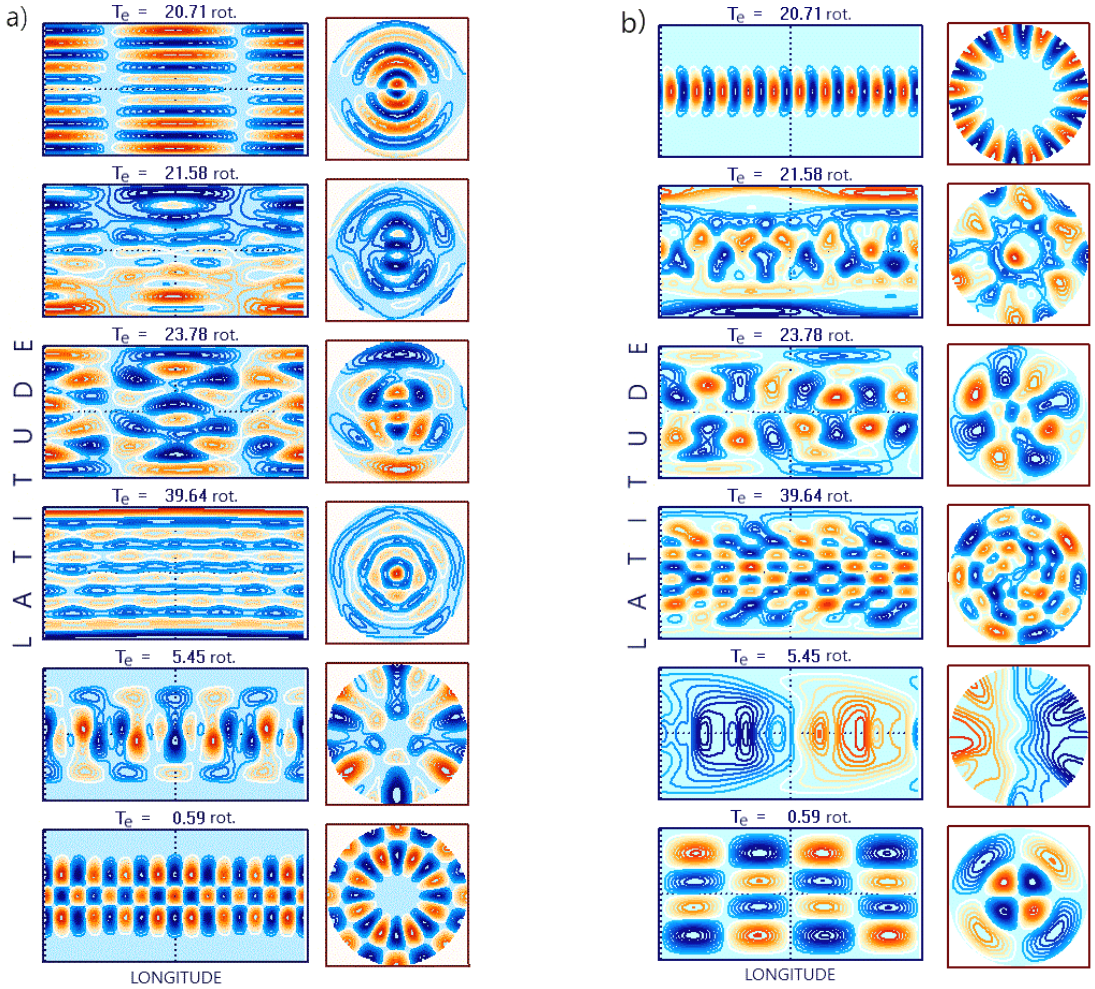

Figure 2. Spatial distributions of the fastest growing normal modes $\psi_0'(\lambda, \mu) = \sum_\gamma \psi_\gamma Y_\gamma(\mu, \lambda)$ (*a*); $\chi_0'(\lambda, \mu) = \sum_\gamma \chi_\gamma Y_\gamma(\mu, \lambda)$ (*b*) at different magnetic field strengths α_1=0.0, α_1=0.0035, α_1=0.035, α_1=0.35, α_1=3.5, α_1=35 (from top to bottom); T_b is the time of an *e*-fold increase in the normal mode amplitude

Table 3

The same as in Table 1 for the differential rotation parameters a = 0.2, f=0.2, and T_0=500.

	α_1=0.0	α_1=0.0035	α_1=0.035	α_1=0.35	α_1=3.5	α_1=35
k=0	T=∞	T=5805.80	T=580.58	T=58.05	T=4.86	T=0.58
k=0.001	T=1782.83	T=1456.64	T=225.03	T=49.31	T=3.2	T=0.26
k=0.005	T=9.56	T=9.58	T=9.93	T=5.80	T=0.47	T=0.04
k=0.01	T=3.27	T=3.33	T=4.07	T=2.34	T=0.24	T=0.02

Table 4

The same as in Table 2 for the differential rotation parameters a=0.2, f=0.2, and T_0=1000, for each k value: in the top row, for N=13; in the bottom row, for N=15.

	α_1=0.0	α_1=0.0035	α_1=0.035	α_1=0.35	α_1=3.5	α_1=35
k=0	T=∞ T=∞	T=5926.23 T=3300.99	T=592.62 T=330.09	T=59.26 T=33.0	T=4.89 T=3.3	T=0.59 T=0.33
k=0.001	T=640.65 T=17201.1	T=610.5 T=948.12	T=209.66 T=186.45	T=49.43 T=30.74	T=3.23 T=2.03	T=0.27 T=0.15
k=0.005	T=9.47 T=4.81	T=9.49 T=4.92	T=9.83 T=6.20	T=5.80 T=5.87	T=0.47 T=0.36	T=0.04 T=0.03
k=0.01	T=3.26 T=1.54	T=3.32 T=1.56	T=4.06 T=1.71	T=2.34 T=2.68	T=0.24 T=0.19	T=0.02 T=0.01

increase in the amplitude of differential rotation anomalies and an increase in the magnetic field in the range 1000–10000 G in all cases lead to a rapid growth in flow instability. The e-folding time of perturbations is reduced by more than an order of magnitude. The increase in the amplitude of differential rotation anomalies is most pronounced in the range k=0.01–0.001. A weak magnetic field stabilizes the flow. This supports the results of numerical calculations performed in [Mordvinov et al., 2019]. The dependence of the instability growth rate on the amplitude of mean flow anomalies yet still turns out to be stronger.

SPATIAL STRUCTURE OF NORMAL MODES OF NONUNIFORM MEAN FLOW

To study the dependence of the spatial structure of normal modes on external forcing, we employ a simpler geostrophic flow model without a magnetic field. Introducing a magnetic field significantly complicates the problem and is not entirely justified since the amount of information on large-scale magnetic field structures and its interpretation are insufficient to compare with the calculation results.

Our task is to calculate the normal modes and to analyze them for the mean flow whose main feature is quasistationary formations — an axisymmetric polar cyclonic vortex and an anticyclonic vortex in midlatitudes. Such a configuration is close to the configuration of flows in Earth's stratosphere. In [Mordvinov and Zorkaltseva, 2022], we drew attention to the fact that axisymmetric perturbations resembling torsional oscillations appear among the most unstable modes of such flows.

As in the previous section, we use a simple geostrophic model in the calculations

$$\frac{\partial(L\psi)}{\partial t} = -\frac{1}{R^2} J(\psi, \Delta\psi) - \frac{2\Omega}{R^2}\frac{\partial\psi}{\partial\lambda} - \\ -r\Delta\psi - K\Delta^3(\Delta\psi) - f(\psi), \qquad (19)$$

where R is the Earth radius.

By linearizing the equation, expanding it in spherical harmonics, and representing perturbations as normal modes, we derive an equation for eigenvalues and eigenvectors of a matrix characterizing the interactions of normal modes with the mean flow,

$$A_{\gamma\gamma'}\psi_{\gamma} = \sigma'\psi_{\gamma'}, \qquad (20)$$

where

$$A_{\gamma\gamma'} = \frac{1}{k_{n'}\Omega}\left\{\int_S Y_{\gamma'}^* J(Y_{\gamma}, G_n)dS\right\} + \\ +\delta_{\gamma\gamma'}\left[i2m' - r_1 n'(n'+1)\right],$$

$$G_n = \Delta\bar{\psi} + k_n\bar{\psi},\ k_n = n(n+1) + F^2,$$

$F \equiv a / L_{\mathrm{D}}$ is the Froude number.

Components of the eigenvectors are the coefficients of expansion in spherical harmonics.

In the previous section, we have used quadratures to calculate the double integrals included in the expressions for elements of the matrix $A_{\gamma\gamma'}$. Now we adopt the method of interaction coefficients, which is often employed in numerical simulation of the general atmospheric circulation. To do this, we expand the stream function $\bar{\psi}$ of mean flow in spherical harmonics $\bar{\psi}(\lambda, \mu) = \sum_{\gamma''}\bar{\psi}_{\gamma''}Y_{\gamma''}(\mu, \lambda)$ and substitute $G_n = \Delta\bar{\psi} + k_n\bar{\psi} = \sum_{\gamma''}^{N}\bar{\psi}_{\gamma''}(k_n - k_{n''})Y_{\gamma''}$ in the expression for the operator. The formula for calculating the $A_{\gamma\gamma'}$ matrix components takes the form

$$A_{\gamma\gamma'} = \frac{1}{\Omega}\left\{\sum_{\gamma''}^{N}\bar{\psi}_{\gamma''}\left(\frac{k_n - k_{n''}}{k_{n'}}\right)\int_S Y_{\gamma'}^* J(Y_{\gamma}, Y_{\gamma''})dS\right\} + \\ +\delta_{\gamma\gamma'}\left[i2m' - r_1 n'(n'+1)\right] \qquad (21)$$

In this expression, the scalar product

$$\int_S Y_{\gamma'}^* J(Y_{\gamma}, Y_{\gamma''})dS = \\ = \frac{i}{2}\int_S Y_{\gamma'}^*\left[m_{\gamma}Y_{\gamma}\frac{\partial Y_{\gamma''}}{\partial\mu} - m_{\gamma''}Y_{\gamma''}\frac{\partial Y_{\gamma}}{\partial\mu}\right]dS \qquad (22)$$

is a mathematical expression for the mechanism of nonlinear resonant interaction between three spherical functions (triads). Analytical calculations of the interaction coefficients allow us to obtain rules for selecting non-zero values of the coefficients, which significantly simplifies the problem-solving algorithm. In the calculations, we use the interaction coefficients for N=13 and N=15 of spherical harmonics in the expansion, as in the first part of the work.

We will set the mean flow structure in the form of a sum of Gaussians. $\bar{\psi} \sim \pm\exp\{-kp^2\}$. Here p is the orthodromy — the distance between the center of the vortex and an arbitrary point on the sphere; k is the coefficient characterizing the width of the Gaussian. In radians, the width of the Gaussian is related to the coefficient k by the ratio $\Delta = 1/\sqrt{2k}$.

Calculations have shown that with the selected modeling parameters all normal modes of the polar cyclone at a Gaussian width >50° (>25° from the pole) are damped; and at a width >77° (>39° from the pole), two modes are the least damped — axisymmetric (n=6, m=0) and dipole (n=1, m=–1). Spectra of the least damped modes and their spatial structure in stereographic and cylindrical projections at a cyclone width of 77° are depicted in Figure 3. Thus, we can assume that the axisymmetric torsional oscillations observed in the atmosphere are the least damped normal modes of the polar cyclonic vortex.

The axisymmetric oscillations also turn out to be quite stable when numerically calculated. Figure 4, *a* presents the results of calculation of the evolution of an axisymmetric normal mode over 28 days with numerical extrapolation at a time step of 0.01 day. The normal mode was taken as initial conditions. At each time step, the disturbance inter acted with the polar cyclone. Panel *b* shows, for comparison, the results of calculation of the evolution of the dipole

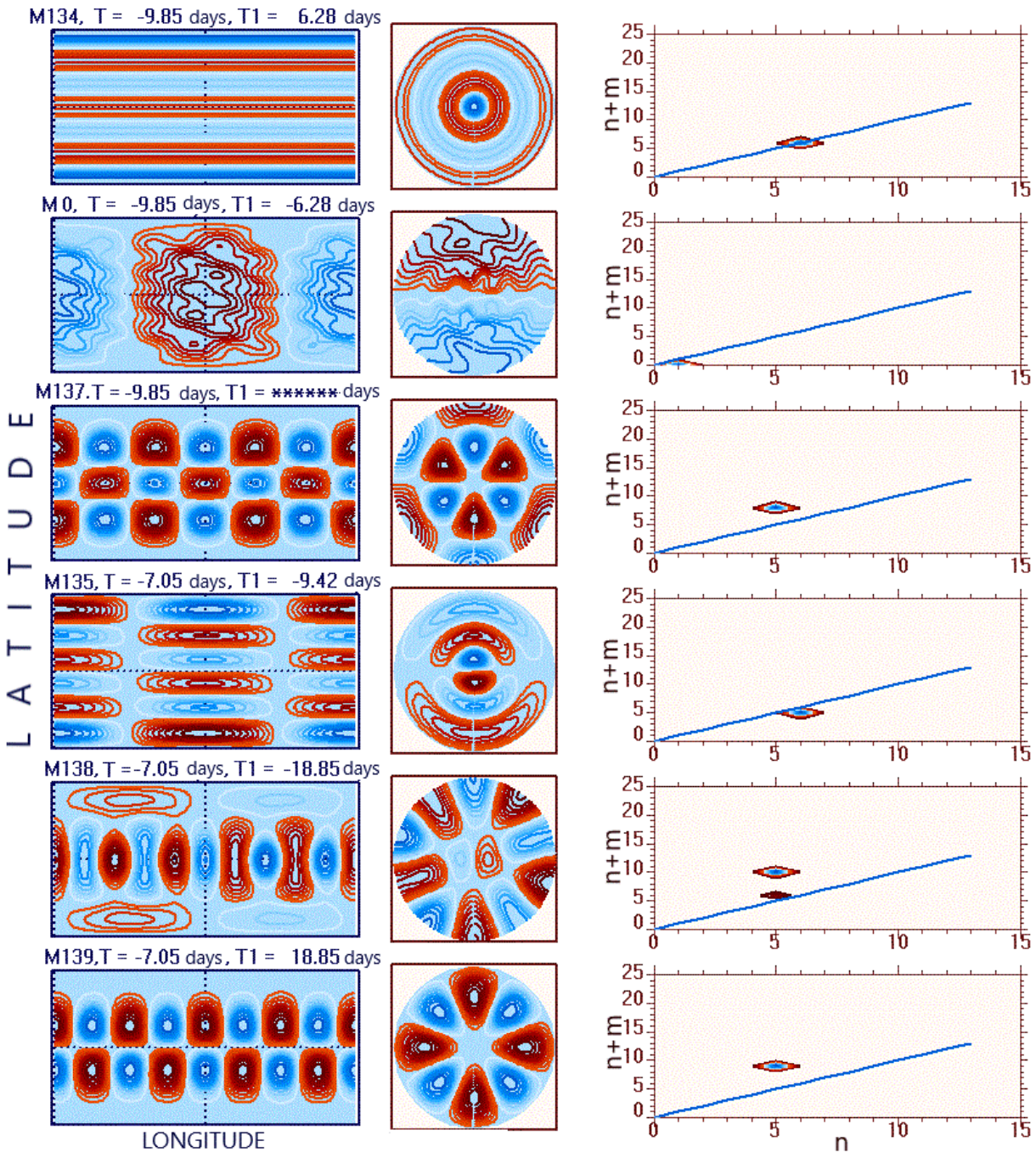

Figure 3. Spatial structure of the least damped normal modes of the polar cyclone in cylindrical (left) and stereographic (center) projections. The time T determines the e-folding time of exponential damping of the mode, $T1$ is the period of oscillation of the mode, the sign before $T1$ is the direction of the transfer of the mode to the east (+) or to the west (–). In relative units (from –0.9 to +0.9), stream function isolines are plotted: blue isolines correspond to negative values; red, to positive ones. On the right is the spectral composition of normal mode: the X-axis is the degree of the spherical function n; the Y-axis, the sum $n+m$, where m is the zonal wavenumber. The straight blue line indicates axisymmetric harmonics at $m=0$

mode over the same time period. It is clearly seen how quickly the dipole evolved and a characteristic spiral structure was formed instead. Statistical processing of observational data over long time periods does reveal such structures. Unfortunately, the oscillation period (6.28 days) for axisymmetric and dipole modes also appears to be shorter than both the torsional oscillation period (~15 days) and the oscillation period of two-dimensional Rossby waves [Branstator, Held, 1995]. The reason for the differences might be the too simple geometry of the mean flow and/or the modeling parameters adopted in calculations.

Let us see how normal modes will change when an anticyclone appears at midlatitudes. Figure 5 presents the results of calculations of normal modes for the flow caused by the superposition of a polar cyclonic vortex and an anticyclonic vortex centered at 60° N. The stream function was given by the sum of two Gaussians

$$\overline{\psi} = 0.5\exp\left\{-kp^2\right\} - 0.35\cdot 0.2l\exp\left\{-klp^2 l\right\}.$$

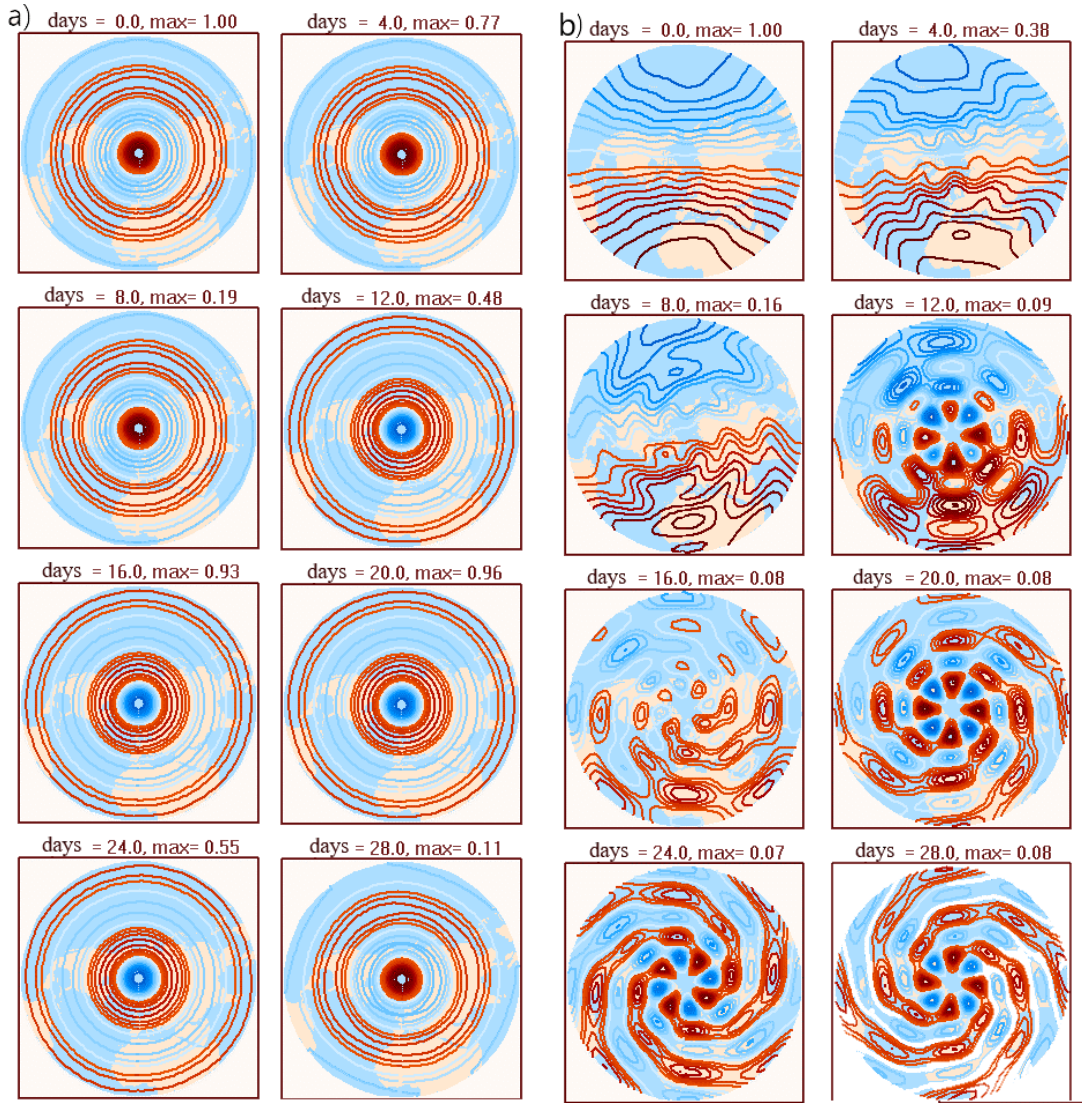

Figure 4. Results of numerical time extrapolation of axisymmetric (*a*) and dipole (*b*) normal modes. The extrapolation time interval is 28 days, the time step for numerical calculation is 0.01 day. The time interval between frames (from left to right and from top to bottom) is 4 days. In relative units from –0.9 to +0.9 in the stereographic projection, isolines of the stream function of normal modes are mapped

The *l* parameter varied from 0 to 5 (from top to bottom). As *l* increased from 1 to 5, the amplitude of the anticyclonic vortex increased five times, while the width of the anticyclone decreased. Both contributed to the increasing instability of the flow. Figure 5, *d* illustrates distributions of stream functions $\bar{\psi}$. Figure 5, *a*, *b* shows modes with the largest increments in cylindrical and stereographic projections; Figure 5, *c*, spectra of normal modes.

It can be seen how the structure of the fastest growing modes becomes more complex with an increase in amplitude and a decrease in the width of the anticyclone. For the polar cyclone, the axisymmetric mode is the least damped. In the most unstable flow configuration with a strong anticyclone, the fastest growing normal mode is the sum of three spherical harmonics (see Figure 5, *b*, bottom panel).

Figure 6 exhibits spectra of normal modes: *a* — for N=13 (corresponding to Figure 5); *b* — for N =15.

Colors of the isolines change from dark blue to light blue with enhanced mean flow instability, i.e. with increasing anticyclone amplitude (from top to bottom in Figure 5). At N=13, the spectrum of rapidly growing modes is limited to degrees of harmonics 5 and 7. When the resolution is increased to N=15, spherical functions with degrees 3 and 4 appear in the spectrum. At the same time, the growth rates of the most unstable harmonics become lower, i.e. the flow turns out to be more stable.

CONCLUSION

In the first part of the work, we have presented the results of numerical experiments with the magnetohydrodynamic model of shallow water, which were aimed at assessing the degree of the magnetic field effect on the development of instabilities of a stationary flow with a frozen-in magnetic field. The magnetic stream function was assumed to be proportional to the stream function

of mean flow, which is the sum of the stream function of differential rotation and spherical harmonic of the sixth degree. The friction force was provided by the Rayleigh friction and the hyperviscosity of the third degree. In the assumed approximations, we have calculated normal modes of mean flow with a frozen-in magnetic field. In the stream function expansion, we have taken into account 13 and 15 spherical harmonics. Normal mode computing has confirmed our earlier result, obtained in a numerical experiment, that effects of weak and strong magnetic fields on differential rotation instability differ. A weak magnetic field stabilizes the development of instability, while a strong one, on the contrary, enhances it. Resulting dependences of the instability increment on the mean magnetic field strength are consistent with the statements about the stabilizing role of the magnetic field [Mishin, Tomozov, 2014] and with the conclusions that instabilities are enhanced when a magnetic field is included in model calculations [Cally et al., 2003; Dikpati, Gilman, 2001; Gilman et al., 2007; Gilman, Fox, 1997]. Azimuthal differential rotation inhomogeneities in all the cases contributed to the development of instabilities.

In the second part of the work, the object of the study was the spatial structure of normal modes. We explored the possibility of explaining torsional oscillations in the terrestrial and solar atmospheres by normal modes. To simplify the calculations, we ignored the magnetic field effect on the flow, i.e. the model corresponded more closely to the conditions of Earth's atmosphere.

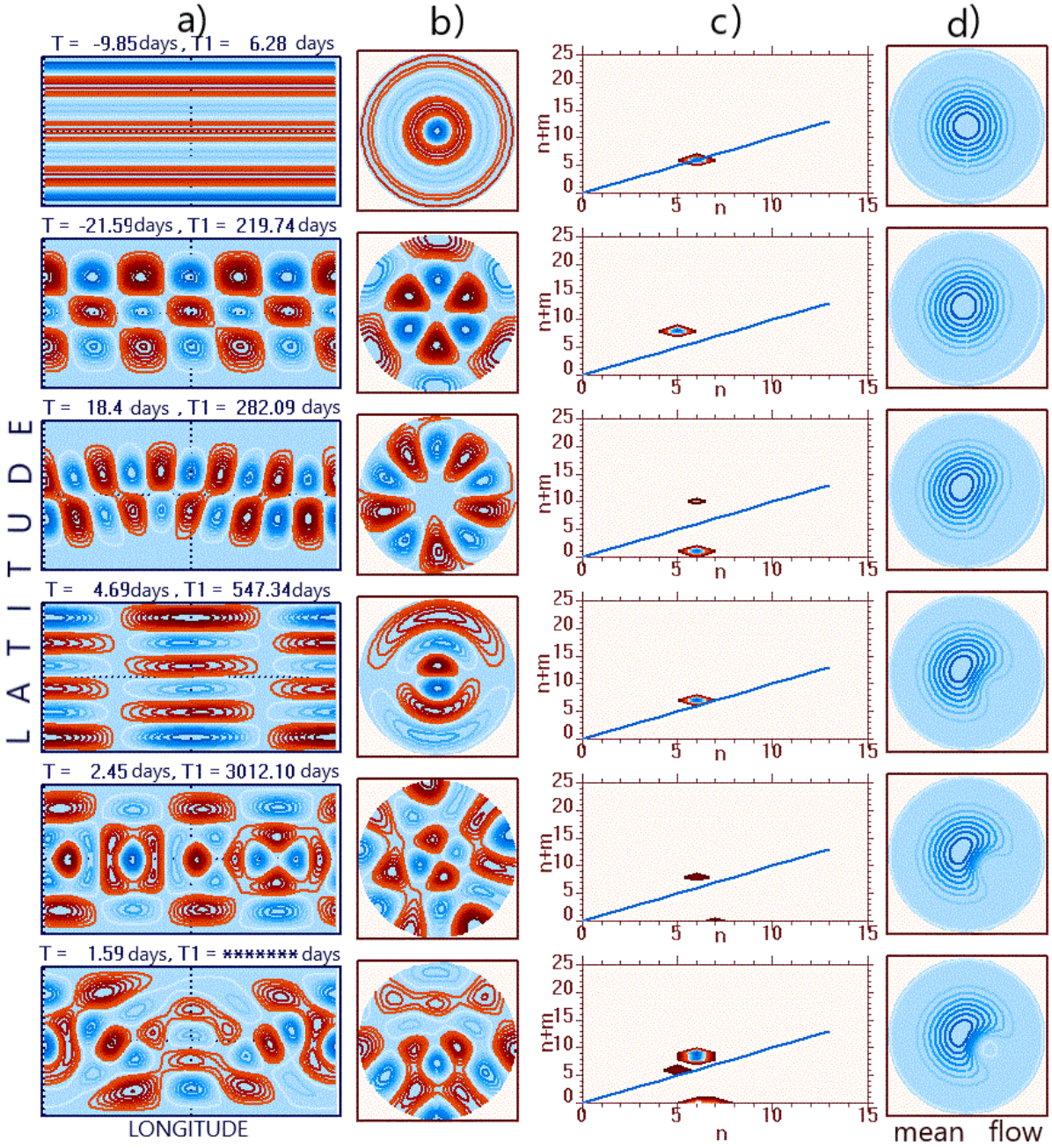

Figure 5. Spatial structure of normal modes with the largest increments in cylindrical (*a*) and stereographic (*b*) projections, spectra of normal modes (*c*), and mean-flow configuration (*d*) at different anticyclone parameters

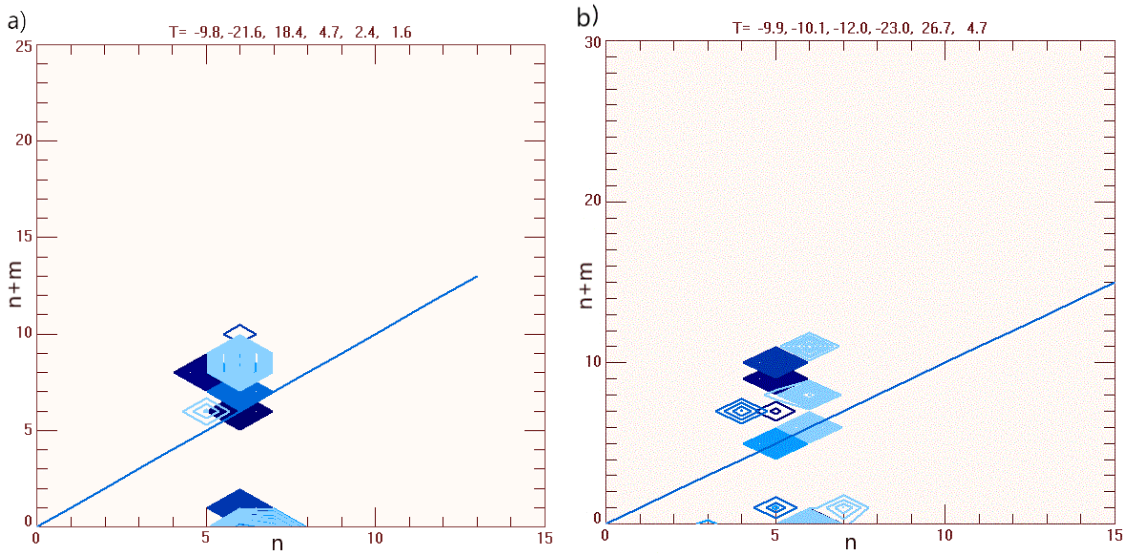

Figure 6. Spectra of normal modes with the largest increments for the polar cyclone + anticyclone flow, on the left — for N=13 (as in Figure 5), on the right — for N=15. Amplitudes of the anticyclone varied from minimum to maximum (dark blue and light blue isolines)

The main component of the mean flow was an axisymmetric polar vortex. Such a flow configuration is typical for Earth's atmosphere and, probably, for the Sun's atmosphere. Calculations have shown that the large-scale cyclonic vortex over the pole is stable, which was to be expected, and two modes were the least damped — the axisymmetric mode resembling torsional oscillations and the horizontal dipole mode. Large-scale mean flow anomalies (anticyclonic vortex at midlatitudes of the Northern Hemisphere) disrupted the stability of the polar vortex. The axisymmetric and dipole modes remained weakly damped, but rapidly growing normal modes appeared, which generally have a more complex spatial structure.

The main results are of a more qualitative nature since the calculations of the increments of normal modes and, moreover, their spatial structure depend very strongly on the adopted assumptions, the structure of the model, configurations of the mean flow and the mean magnetic field. To make quantitative conclusions about the structure of normal modes and growth increments of normal modes, all these parameters should be clarified.

The work was financially supported by the Ministry of Science and Higher Education of the Russian Federation (Subsidy No. 075-GZ/Ts3569/278).

REFERENCES

Altrock R., Howe R., Ulrich R. Solar torsional oscillations and their relationship to coronal activity. *American Astronomical Society, SPD Meeting, BAAS 38*. 2006, vol. 38, p. 258. http://adsabs.harvard.edu/cgi-bin/nph-bib_query?bibcode=2006SPD....37.3203A.

Branstator G., Held I. Westward Propagating Normal modes in the presence of stationary background waves. *J. Atmos. Sci.* 1995, vol. 52, pp. 247–262.

Bumba V. Large-scale magnetic fields on the Sun. *Solar Activity Problems*. Moscow, Mir Publ., 1979, pp. 50–74. (In Russian).

Bumba V., Howard R. Large-scale distribution of solar magnetic fields. *Astrophys. J.* 1965, vol. 141, no. 4, pp. 1502–1512.

Bumba V., Makarov V. Background magnetic fields on the Sun. *Solar Magnetic Fields. I. Corona: Proc. XIII Consultative Conference on Solar Physics*. Novosibirsk, Nauka Publ., 1989, vol. 1, pp. 51–71. (In Russian).

Cally P.S., Dikpati M., Gilman P.A. Three-dimensional magnetoshear instabilities in the solar tachocline. *Monthly Notices of the Royal Astron. Soc. Papers*. 2003, vol. 339, iss. 4, pp. 957–972.

Danilov S.D., Gurarii D. Quasi two-dimensional turbulence. *Physics-Uspekhi*. 2000, vol. 170, iss. 9, pp. 921–969.

Dikpati M., Gilman P.A. Analysis of hydrodynamic stability of solar tachocline latitudinal differential rotation using a shallow-water model. *Astrophys. J. Papers*. 2001, vol. 551, pp. 536–564. DOI: 10.1086/320080.

Dikpati M., Gilman P.A. A shallow-water theory for the Sun's active longitudes. *Astrophys. J*. 2005, vol. 635, iss. 2, pp. L193–L196.

Dymnikov V., Filatov A. Sustainability of large-scale atmospheric processes. *Computing Mathematics Department AS USSR*. Moscow, 1988, pp.1–140. (In Russian).

Dymnikov V., Skiba Yu. Barotropic instability of zonal asymmetric atmospheric flows. *Computing Processes and Systems*. Iss. 4. Moscow, Nauka Publ., 1986, pp. 63–104. (In Russian).

Fournier D., Gizon L., Hyest L. Viscous inertial modes on a differentially rotating sphere: Comparison with solar observations. *Astron. Astrophys*. 2022, vol. 664, pp. 1–16. DOI: 10.1051/0004-6361/202243473.

Gill A. *Dynamics of atmosphere and ocean*. In 2 vol. Moscow, Mir Publ., 1986, vol. 2, 415 p.

Gilman P.A. Stability of baroclinic flows in a zonal magnetic field. Part 1–3. *J. Atmos. Sci*. 1967, vol. 24, no. 2, pp. 101–143.

Gilman P.A., Fox P.A. Joint instability of latitudinal differential rotation and toroidal magnetic fields below the solar convection zone. *Astrophys. J*. 1997, vol. 484, no. 1, pp. 439–454.

Gilman P.A., Dikpati M., Miesch M.S. Global MHD instabilities in a three-dimensional Thin-Shell Model of solar tachocline. *Astrophys. J. Suppl. Ser. Papers*. 2007, vol. 170, pp. 203–227. DOI: 10.1086/512016.

Kitchatinov L.L., Rüdiger G. Stability of latitudinal differential rotation in stars. *Astron. Astrophys*. 2009, vol. 504, no. 2, pp. 303–307.

Large-Scale Dynamic Processes in the Atmosphere. Moscow, Mir Publ., 1988, 430 p. (In Russian).

Marchuk G., Agoshkov V., Shutyaev V. Adjoint Equations and Perturbation Algorithms in Applied Problems. *Computing Processes and Systems.* Moscow, Nauka Publ., 1986, 272, pp. 5–62. (In Russian).

Miesch M.S. Large-scale dynamics of the convection zone and tachocline. *Living Reviews in Solar Physics*. 2005. Vol. 2, no. 1. P. 1–139.

Mishin V., Tomozov V. Manifestations of Kelvin-Helmholtz instability in the solar atmosphere, solar wind and Earth's magnetosphere. *Solar-Terr. Phys*. 2014, iss. 25, pp. 10–20. (In Russian).

Mordvinov V.I., Zorkaltseva O.S. Normal Mode as a Cause of Large-Scale Variations in the Troposphere and Stratosphere. *Izvestiya, Atmospheric and Oceanic Phys.* 2022, vol. 58, no. 2, pp. 140–149.

Mordvinov V., Devyatova E., Tomozov V. Hydrodynamic instabilities in a tachocline due to layer thickness variations. *Solar-Terr. Phys*. 2012, iss. 20, pp. 3–8. (In Russian).

Mordvinov V., Devyatova E., Tomozov V. Hydrodynamic instabilities in the tachocline due to layer thickness variations and mean flow inhomogeneities. *Solar-Terr. Phys*. 2013, iss. 23, pp. 3–12. (In Russian).

Mordvinov V., Latysheva I. General circulation theory of the atmosphere, variability of large-scale motions. *Irkutsk, izdatelstvo IGU*, 2013, 193 p. (In Russian).

Mordvinov V.I, Olemskoy S.V., Latyshev S.V. Influence of mean magnetic field and magnetic field of the velocity disturbances on the development of hydrodynamic instabilities in tachocline. *Proc. SPIE 11208, 25th International Symposium on Atmospheric and Ocean Optics: Atmospheric Physics*, 1120803 (18 December 2019). 2019. DOI: 10.1117/12.2538285.

Tikhomolov E.M. Large-scale vortical flows and penetrative convection in the Sun. *Nuclear Physics A.* 2005, vol. 758, no. 1. pp. 709–712.

Zorkaltseva O.S., Mordvinov V.I., Devyatova E.V., Dombrovskaya N.S. Method For Calculating Torsional Oscillations in Earth's Atmosphere from NCEP/NCAR, MERRA-2, ECMWF ERA-40, AND ERA-INTERIM. *Solar-Terr. Phys.* 2019, vol. 5, iss. 1, pp. 69–76. DOI: 10.12737/stp51201910.

Original Russian version: Mordvinov V.I., Devyatova E.V., Tomozov V.M., published in Solnechno-zemnaya fizika. 2023. Vol. 9. Iss. 4. P. 134–146. DOI: 10.12737/szf-94202315.

How to cite this article

Mordvinov V.I., Devyatova E.V., Tomozov V.M. Influence of the magnetic field and the mean flow configuration on spatial structure and growth rate of normal modes. *Solar-Terrestrial Physics.* 2023. Vol. 9. Iss. 4. P. 123–135. DOI: 10.12737/stp-94202315.